THE JOURNAL OF PHYSICAL CHEMISTRY B

ARTICLE

pubs.acs.org/JPCB

Spontaneous Formation of a Vesicle Multilayer on Top of an Exponentially Growing Polyelectrolyte Multilayer Mediated by Diffusing Poly-L-lysine

Norma Graf, Elsa Thomasson, Alexander Tanno, Janos Vörös, and Tomaso Zambelli*

Laboratory of Biosensors and Bioelectronics, Institute for Biomedical Engineering, ETH Zürich, Gloriastrasse 35, 8092 Zürich, Switzerland

Supporting Information

ABSTRACT: We observed the spontaneous formation of vesicle-multilayers on top of a polyelectrolyte multilayer (PEM). By varying the thickness of underlying PEM (uPEM) it was possible to tailor the amount of adsorbing liposomes. Thereby, the loading capacity could be increased up to 17 times with respect to a monolayer of vesicles for an uPEM of 50.5 bilayers. We, furthermore, proved that the formation of the vesicle multilayer is due to the ability of poly-L-lysine to diffuse within the uPEM. This method could be interesting for applications in sensors and drug delivery systems where the increase in loading capacity is highly desired.

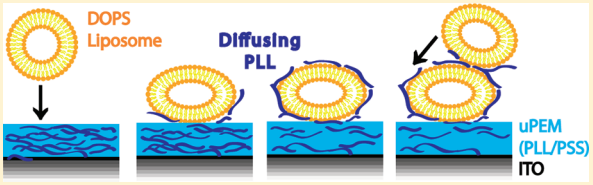

1. INTRODUCTION

Liposomes are one of the most promising systems for encapsulation and delivery of substances due to a set of critical advantages over competing methods. Not only are they biocompatible and can be filled with a broad range of substances, they can also be mass produced from natural ingredients.[1−3]

Immobilization of liposomes in a matrix is an important element toward the preservation of the liposomes' structural stability and the protection of them from unwanted reactions with the external environment. Michel and co-workers first combined these advantages of embedding liposomes with a strategy for stimulated release and demonstrated the temperature-triggered release of fluorescent dye from liposomes embedded in a film of poly-L-glutamic acid and poly-(allylamine hydrochloride) (PGA-PAH).[4,5]

However, the incorporation of these vesicles into polyelectrolyte multilayers (PEMs) required stabilizing the liposomes with a layer of poly-L-lysine (PLL) in an extra step prior to adsorption.[4−9] Usually, negatively charged vesicles strongly deform upon adsorption to a positively charged substrate, caused by electrostatic forces. Thereby, the membrane curvature at the edge becomes higher, inducing lipid bilayer formation.[10] Yet, recent investigations showed that vesicles made of 100% negatively charged dioleoylphosphatidylserine (DOPS) lipids adsorbed on PLL and polystyrene sulfonate (PSS) remained intact.[11] This was because the negative charges of the lipids were compensated by the migration of the PLL chains from the uPEM up to the liposomes, avoiding liposome deformation. As a result, the liposomes did not flatten out on the oppositely charged substrate but maintained their natural, more spherical shape which reduced the driving force for vesicle rupture.

Surface-based drug delivery systems are gaining increased attention as new drug administration concepts. Instead of the drug being distributed in solution, it is embedded in a functional coating, enabling a well controlled contact of surrounding cells to the incorporated drug.[12] When these drug delivery systems or surface-based sensors rely on the release of substances from liposomes they often suffer from poor loading capacity.

One option to increase the loading capacity of such a liposome-based encapsulation system is to immobilize the vesicles on the surface not only in one single layer but in a three-dimensional fashion. One example is the proteosome multilayer structure presented by Graneli et al.[13,14] where single-stranded-DNA (ss-DNA) functionalized vesicles were linked to the complementary ss-DNA modified gold substrate via specific DNA hybridization. Then, excess cholesterol DNA was added to the first immobilized vesicle layer to facilitate the coupling of the second vesicle layer. This procedure was then repeated to get a multilayered vesicle structure on the surface.

Another option is the Zr-mediated liposome multilayer of Bürgel et al.[15] By sequential injection of vesicles and multivalent zirconium ions as linkers, they succeeded in constructing three-dimensional phospholipid vesicle constructs. This procedure increased the sensor's loading capacity in a fluorescence-based biomolecular binding assay.

These 3D vesicle constructs could play a key role in the development of sensing devices with increased loading capacity and sensitivity. To keep such a liposome-based device as simple as possible, it is desirable that the vesicles arrange spontaneously and quickly in a three-dimensional construct without adding any linkers or mediators.

We describe here a method to create such "spontaneous 3D vesicle constructs" on PLL/PSS multilayers. We chose PLL as

Received: July 14, 2011
Revised: September 9, 2011
Published: September 19, 2011

polycation because of its throughout incestegated ability to diffuse within an exponentially growing multilayer[16] and to stabilize adsorbing vesicles on top of the layers.[11] DOPS vesicles were adsorbed on different amounts of PLL/PSS bilayers. We demonstrate that the thickness of the 3D-liposome-arrangement increases with an increasing underlying PEM (uPEM). We show that the diffusion of PLL enabled the multilayer construction by acting as a "self-organizing-glue" for vesicle multilayer formation. The results show that the underlying PLL/PSS multilayer serves as a reservoir for the PLL and, therefore, for the 3D-liposome arrangement.

2. MATERIALS AND METHODS

Substrates. All experiments were performed on indium tin oxide (ITO) coated glass, produced by MicroVacuum (Hungary) because the chosen PEM homogeneously covers this surface already at a small number of bilayers.

Polyelectrolytes. PLL: poly-L-lysine hydrobromide, Sigma Aldrich P7890, MW = 24000. PSS: poly(sodium 4-styrene sulfonate), Sigma Aldrich 24,305, MW = 70000. These were dissolved in 150 mM NaCl solution. $(PLL/PSS)_n$ means n layer pairs of the polyelectrolyte couple PLL and PSS. The PEM directly on the substrate is denoted as uPEM. The vesicles were adsorbed onto the uPEM. To be able to image the system by means of atomic force microscopy (AFM), the vesicles on the uPEM were additionally covered by a protection layer of $(PLL/PGA)_2$. PGA: poly-L-glutamic acid (PGA, SIGMA). The integrity of the vesicles upon the adsorption of the covering layer has already been confirmed earlier.[11]

Vesicles. All of the lipids were dissolved in chloroform and stored at −20 °C. Vesicles consisting of 100 wt % DOPS were used. Five mg of the lipids were dried and rehydrated in 150 mM NaCl at pH 5.5 (no buffer used). Then, the suspensions were each extruded through a double-stacked polystyrene membrane with a pore size of 200 nm. The extruded vesicles were diluted to a concentration of 0.5 mg/mL and stored in the fridge for maximum 14 days before use.

The liposomes were characterized at 20 °C with a salt concentration of 150 mM NaCl at pH 5.5 (no buffer used) with respect to their hydrodynamic radius by dynamic light scattering (170 ± 33 nm) and ζ-potential (−45 mV) (Zetasizer, Malvern Instruments, United Kingdom).

Substrate Preparation. The substrates were cleaned by ultrasonication (Elna Transsonic Digital S, Iswork, Singapore) in cleaner (Cobas Integra Cleaner, Roche), isopropanol (puriss., Sigma Aldrich), and ultrapure water (resistivity = 18.2 MΩ/cm, Milli-Q gradient A 10 system, Millipore Corporation) for 10 min in each subsequent solvent. The samples were rinsed with ultrapure water and dried with nitrogen after every cleaning step. Finally, they underwent UV/ozone cleaning (Uvo Cleaner 42−220, Jelight Company, USA) for 30 min prior to spraying.

Spraying Method. The spraying process as described previously[17] has been automated in our laboratory by a home-built spraying robot.[11] The custom-made program first wets the substrate with 150 mM NaCl solution for 5 s. After a pause of 5 s the PLL solution (0.5 mg/mL) was sprayed for 5 s. After a pause of 15 s the substrate was rinsed with buffer or 150 mM NaCl solution for 5 s.[18] After another 5 s break, the PSS solution (0.5 mg/mL) was sprayed for 5 s, followed by 15 s pause and rinsing of the substrate with buffer or 150 mM NaCl solution for 5 s. This procedure was repeated as many times as needed (n) in order to obtain a $(PLL/PSS)_n$-PLL multilayer. The PEM coated samples were stored at 4 °C in 150 mM NaCl solution for maximal 2 days until use.

Quartz Crystal Microbalance (QCM). The QCM measurements were carried out with a QCM system from Q-Sense (Sweden).[19] Briefly, QCM measures the changes in the resonance frequency (Δf) of a quartz crystal when material is adsorbed onto it. The quartz crystal was excited at its fundamental frequency (about 5 MHz) and at the third, fifth, and seventh overtones (n). A decrease in $\Delta f/n$ is, to a first approximation, linearly related to an increase of the mass coupled to the oscillating crystal. Importantly, in the case of liposomes, the measured mass increase includes water coupled to the film inside the liposomes. Upon vesicle rupture, water is released. This can be detected by QCM. Shortly before mounting into the QCM flow cell, the uPEM-covered quartz crystal was rinsed with ultrapure water and dried with nitrogen followed by rehydration in 150 mM NaCl solution within a few minutes. This procedure assured that no salt crystals formed upon drying the samples. The vesicle solution (0.5 mg/mL) was then injected and incubated until a saturation of frequency shift was observed but at least for 30 min. After that, the flow cell was rinsed with 150 mM NaCl solution. For each measuring point, 3 experiments were performed and the average was then plotted. The standard deviation was included in the plots for the calculated ratios.

AFM. We used the Nanowizard I BioAFM (JPK Instruments, Berlin, Germany) with Mikromasch CSC38/noAl cantilevers in contact mode. Samples were mounted in a custom-made Teflon liquid-cell reported in Grieshaber et al.[20] All AFM measurements were performed in liquid (150 mM NaCl). The ITO-coated substrate was sprayed with $(PLL/PSS)_n$-PLL, kept in 150 mM NaCl, and gently scratched with the tip of a screw driver to determine the thickness of the films. Then, the vesicles were added for 30 min and the flowcell was rinsed for 7 times with 400 μL NaCl (150 mM). Subsequently an extra layer of $(PLL/PGA)_2$ was added to faciliate the imaging of the vesicles. After that, the sample was again gently scratched with the tip of a screw driver, in order to find the height after vesicle adsorption.

Images of 100 × 100 μm^2 were taken before and after the adsorption of the vesicles onto the uPEM (set point ∼1 nN, scan rate 0.6−1 Hz). The images were always taken across an area with a scratch to use the scratch as the baseline for the volume evaluation. The volume of a defined area of 20 × 20 μm^2 next to the scratch were determined using MatLab by the same procedure described before.[21] The values were then plotted against the number of uPEM bilayers. Each data point consists of 3 measurements which were then averaged. The error bar is the standard deviation of the measurements.

3. RESULTS AND DISCUSSION

The first point we investigated was a possible correlation between the amount of uPEMs and the amount of adsorbing vesicles onto it. Therefore, four substrates were prepared with different uPEMs made of 0.5, 9.5, 20.5, and 50.5 bilayers. The samples were then imaged by means of AFM before and after addition of the vesicles onto the uPEMs. The vesicles were let adsorb for a defined time of 30 min to ensure the same conditions for all the samples.

Images and profiles across a scratch of the bare PLL/PSS films are reported in the Supporting Information. The corresponding thicknesses are <1 nm (0.5 uPEM), 55 nm (9.5 uPEM), 270 nm

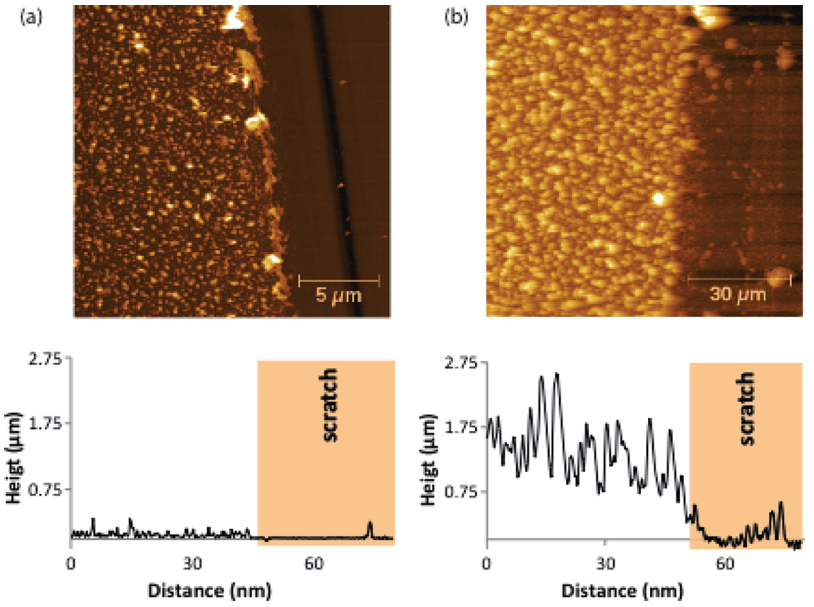

Figure 1. AFM images of the topography across an artificially induced scratch of vesicles adsorbed onto 0.5 (a) and 50.5 (b) uPEMs. Note that for better visualization, a zoom-in of the image for vesicles on 0.5 uPEMs is displayed.

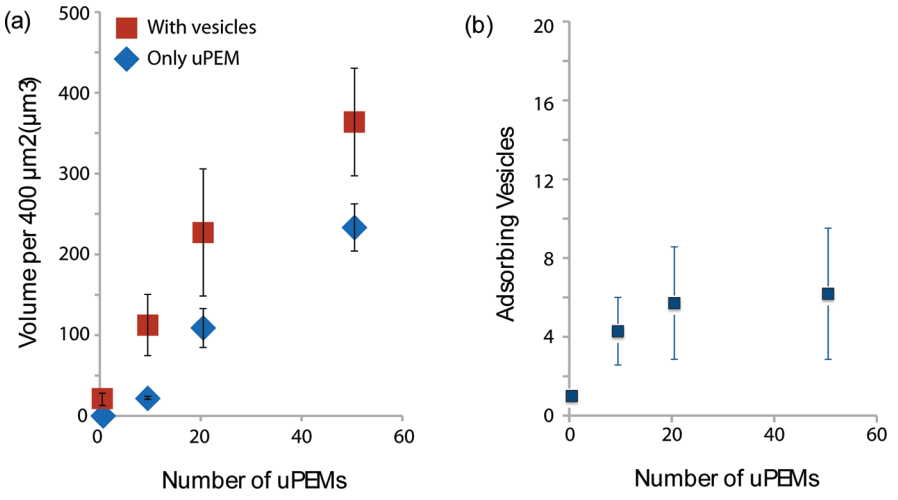

Figure 2. (a) Volumes derived from 20 × 20 μm^2 AFM images of vesicles adsorbed onto 0.5, 9.5, 20.5, and 50.5 uPEMs. (b) Ratios of vesicles adsorbing to the different uPEM substrates.

(20.5 uPEM), and 580 nm (50.5 uPEM). AFM images and cross sections of the adsorption of vesicles on the uPEMs for 30 min are displayed in Figure 1. Two situations were selected: Vesicles adsorbed on top of a single layer of PLL (a) and on 50.5 bilayers (b). A lot of material and many peaks and valleys could be observed for vesicles adsorbed onto 50.5 uPEMs, whereas the cross section for vesicles adsorbed onto 0.5 uPEMs looks much more regular and smoother. The liposomes appeared intact in both cases.

To quantify the vesicle adsorption on the uPEMs, the volume of an 20 × 20 μm^2 area was calculated for each AFM sample before and after the vesicle addition (Figure 2, calculation, see Materials and Methods, AFM). On a single PLL layer, whose volume is considered to be negligibly small, the volume of the adsorbing vesicles was approximately 21 μm^3. The volume for vesicles adsorption onto 9.5, 20.5, and 50.5 uPEMs was found to be 115, 230, and 365 μm^3, respectively. Subtracting the volume of the uPEM results in an additional difference (ΔV) for the vesicle adsorption of 90, 120, and 130 μm^3. The increase in ΔV with increasing uPEMs suggests that there seems to be a correlation between the amount of adsorbing vesicles and uPEM thickness. To evaluate the efficiency of the spontaneous multilayer formation the volume of the adsorbed vesicles for different uPEMs was compared to the volume of a monolayer of vesicles on 0.5 uPEMs. The ratios were found to be 1, 4, 5.5 and 6, respectively (Figure 2b, for calculation, see Materials and Methods, AFM). This means that the loading capacity of the system was increased by a factor of 6 simply by increasing the amount of uPEMs.

However, there seems to be a plateau in vesicle adsorption for uPEMs thicker than 20.5 (Figure 2 b). Since the AFM experiments were carried out at a fixed adsorption time, we checked

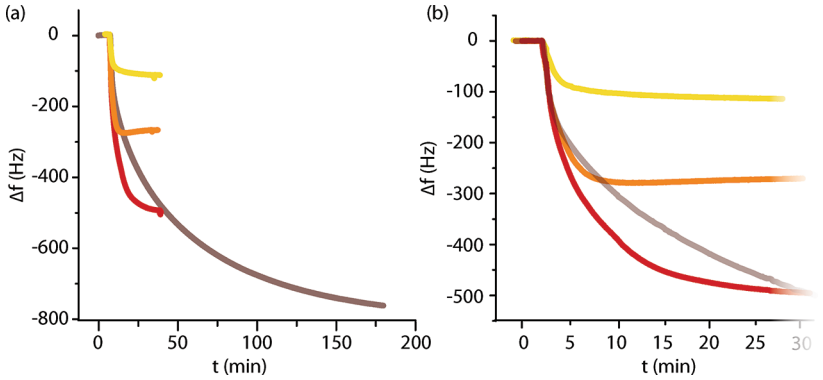

Figure 3. (a) QCM data of vesicles adsorbing onto 0.5, 3.5, 9.5, and 20.5 uPEMs. (b) Zoom-in to the first 25 min, to see the time needed for saturation for vesicles adsorbing onto 0.5, 3.5, and 9.5 uPEMs. The thicker the uPEM underneath, the higher was the saturation frequency. Moreover, saturation time also increased with an increasing amount of uPEMs.

whether the loading capacity can be even further increased if the vesicles were left on the surface for longer times.

The QCM technique allows to follow the adsorption processes in situ. Therefore, another experiment was performed by means of QCM. Vesicles adsorption onto different uPEM with thicknesses of 0.5, 3.5, 9.5, and 20.5 was studied over time. The vesicles were adsorbed until a saturation in frequency shift was established but for a minimum time of 30 min.

Indeed, the trend from the AFM experiments could be confirmed. A bigger frequency shift was observed if the same vesicles were adsorbed to higher amounts of uPEMs for 30 min. However, at 30 min the vesicle adsorption onto 20.5 uPEMs did not saturate yet.

It can actually be noticed that the time for saturation after vesicle adsorption was increasing from 5 min for 0.5 uPEMs, to 10 min for 3.5 uPEMs, to 20 min for 9.5 uPEMs, to more than 2 h and 40 min for 20.5 uPEM (parts a and b of Figure 3).

The frequency shift after saturation was found to be around 100 Hz for 0.5 uPEMs and approximately 280, 500, 750, and 2000 Hz for 3.5, 9.5, 20.5, and 50.5 uPEMs leading to ratios of 1, 2.3, 4, 6.5, and 17 (Figure 4).

This means, in comparison to the adsorbing vesicles in one layer, we have an up to 17-fold increase in loading capacity of our system within 6 h simply by adjusting the underlying amount of (PLL/PSS) couples.

Other multilayer vesicle contructs show an up to 6-fold increase of the loading capacity compared to a single layer, by sequential adsorption of liposomes and linkers within 6 to 8 h.[13−15]

The ratios for 9.5 and 20.5 uPEMs are in a comparable range for the AFM and the QCM measurements (Figure 2b and 4). It can be seen, that for 50.5 bilayers the ratio is much higher for the QCM. This is because the vesicles in the AFM experiement were only adsorbed for 30 min, whereas in the QCM they were adsorbed for more than 6 h. If one looks at the value after 30 min in the QCM data (Figure 3b) one sees that the frequency shift for the adsorption is approximately 500 Hz, leading to a ratio of 5 for 20.5 uPEMs, close to the one obtained by AFM (5.5). However, it is important to note that the two techniques are not completely comparable due to their experimental setup and in particular the dimension of the flow cells.

The AFM and QCM data indicated that there are multilayers of intact vesicles on the uPEMs. Because of its stabilization role as described in Michel et al.,[7] we assumed that PLL abundance is the crucial factor for the creation of spontaneous vesicle multilayers.

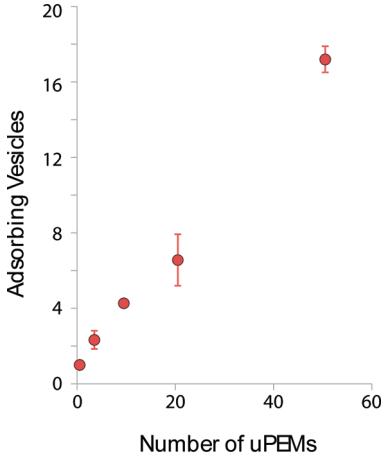

Figure 4. Ratios of vesicle adsorption vs the amount of uPEMs. If the adsorption time is long enough one can get an up to 17-fold increase in loading capacity. The 50.5 point is derived from the QCM curve in Figure 6.

Multilayers consisting of PLL and PSS are exponentially growing.[22] This means, that PLL is able to diffuse in the highly hydrated film as it was demonstrated for the PLL/HA system.[16]

Normally vesicles deform when they adsorb to a oppositely charged surface because of electrostatic interactions between the lipids and the surface. We believe that upon vesicle adsorption the positively charged PLL chains migrate up to the negatively charged vesicles[11] and allow new arriving vesicles to stick on the PLL-vesicle complexes (Figure 5).

This would also explain the increasing saturation time for vesicle adsorption onto thicker uPEMs. Since the uPEM, as well as the vesicle layer on top of the uPEM, becomes thicker, the diffusion distance of PLL to the newly arriving vesicles is significantly growing.

The confirmation of this role of PLL was assessed with QCM: the same vesicles were adsorbed onto 50.5 (PLL/PSS) uPEMs and another 50.5 layered uPEM, which was made of (PLL/PSS)43-(PAH/PSS)7-PLL instead. This combination of PEMs was chosen since the intermediate (PAH/PSS) layer is known to hinder the diffusion of PLL acting as a barrier for it.[16,23−25]

If the increase in vesicle adsorption was due to PLL diffusion, the increase for this setup would be similar to the increase for 0.5 uPEMs, since the amount of PLL that can diffuse is the same in both cases.

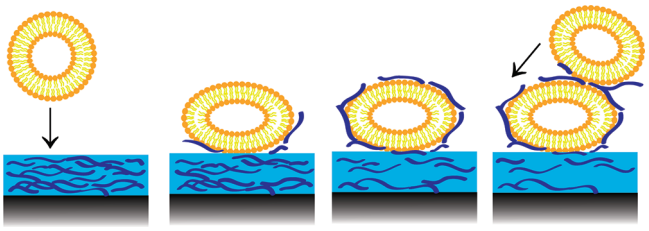

Figure 5. Illustration of the PLL migration to stabilize the vesicles upon adsorption. PLL is able to diffuse up to the vesicle and stabilize it by compensation of the negative charges. This allows the vesicles to remain in a less distorted shape. Then more PLL can migrate up along the vesicles and overcompensate their negative charges. Newly arriving vesicles can then again attach to the now slightly positively charged vesicles.

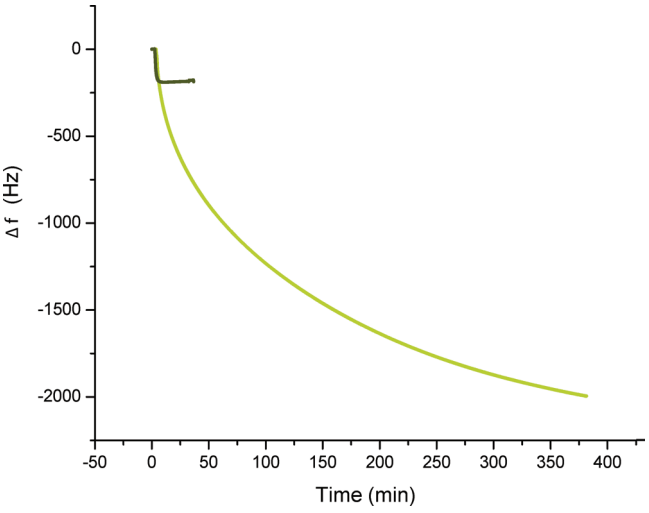

Figure 6. QCM curves for vesicle adsorption onto "normal 50.5 uPEM" made of (PLL/PSS) and onto the "barrier 50.5 uPEM made of $(PLL/PSS)_{43}$-$(PAH/PSS)_7$-PLL.

Figure 6 shows the adsorption curves for vesicles adsorbed onto a "normal" 50.5 uPEM made of (PLL/PSS) and onto the "barrier" 50.5 uPEM. The saturation value for vesicles adsorbed onto $(PLL/PSS)_{43}$-$(PAH/PSS)_7$-PLL was approximately 200 Hz. This is in the range of the increase for 0.5 to 3.5 uPEMs (115 and 270 Hz). The value for vesicles adsorbed onto the "normal 50.5 uPEM" was around 2000 Hz after approximately 6 h.

This shows that the PLL diffusion is indeed crucial for the formation of spontaneous vesicle multilayers. The thicker the uPEM, the larger is the "reservoir" for PLL that can diffuse and migrate and, thereby, allow newly arriving vesicles to remain bound to the surface. This finding was confirmed by a similar experiment carried out by AFM, putting the PSS/PAH barrier at a different position in the PEM. The adsorbed amount of vesicles on $(PLL/PSS)_{34}$-$(PAH/PSS)_7$-$(PLL/PSS)_9$-PLL was 102 μm^3 (Supporting Information) being very close to that on $(PLL/PSS)_9$-PLL (112 μm^3, see Figure 2).

To get a direct proof of the PLL migrating in the vesicle multilayer, fluorescent PLL was used to fabricate the $(PLL/PSS)_{100}$ film, and the subsequent vesicle adsorption was monitored by confocal laser scanning microscopy (CLSM). If the PLL migrated up to the vesicles, the fluorescent PLL should spread over a larger thickness than before vesicle adsorption. For the parameters of our setup, the fluorescent signal of the PLL/PSS film before vesicle adsorption is not an ideal step function, but already spread over 4−8 μm (data not shown), a much bigger value than the actual thickness for 100.5 bilayers derived by AFM (1.2 μm), impeding every further quantitative investigation of the PLL migration. Much thicker uPEMs (>8 μm, approximately 800 uPEMs) would be needed for the CLSM, which could not any more studied by AFM and QCM.

The remaining open question is the correlation between the kinetics of the multilayer formation with the PLL diffusion. Three simultaneous processes lead to the multilayer formation: (a) PLL diffusion in the PLL/PPS film, (b) sticking of the vesicles from the solution to the PLL top layer, and (c) PLL diffusion in the vesicle multilayer. The amount of PLL in the vesicle multilayer should be measured as function of time to determine the rate of each process. Yet, the QCM technique does not allow to extract the amount of of PLL acting as a "glue" in the vesicle multilayer and the amount of attached vesicles from the total adsorbed mass, while the CLSM z-stack has not the sufficient z resolution to follow the PLL diffusion.

4. SUMMARY AND CONCLUSION

We were able to obtain "spontaneous 3D vesicle constructs" with an up to 6-fold increased loading capacity within 30 min and 17-fold after 6 h. We showed that the amount of adsorbed vesicles is dependent on diffusion distance and availability of PLL in the underlying PEM layers.

This is, to our knowledge, the first time that the construction of a vesicle multilayer with different thicknesses could be steered only by the composition and thickness of the underlying PEM film.

These findings might be relevant for surface-based drug delivery applications or sensing devices, where the loading capacity is a key factor.

■ ASSOCIATED CONTENT

Supporting Information. AFM images and cross sections of the bare uPEMs. AFM image and cross sections of the additional barrier experiment with $(PLL/PSS)_{34}$-$(PAH/PSS)_7$-$(PLL/PSS)_9$-PLL and its comparison to $(PLL/PSS)_9$PLL. This information is available free of charge via the Internet at http://pubs.acs.org.

■ AUTHOR INFORMATION

Corresponding Author
*E-mail: zambelli@biomed.ee.ethz.ch.

■ ACKNOWLEDGMENT

This work was supported by the ETH Research Grant ETH-17 08-1. Thanks to Fouzia Boulmedais and Pierre Schaaf (Institut Charles Sadron, Strasbourg, France), to Erik Reimhult (BOKU, Wien), and to Dominik Textor (ETH LBB) for fruitful discussions. Thanks also to Dominik Textor for the construction of the spraying robot and Steven Wheeler (ETH LBB workshop) for technical help. The Germaine de Staël France-Switzerland Project 2011 is acknowledged for financial support.

■ REFERENCES

(1) Mozafari, M. R.; Khosravi-Darani, K. *Nanomaterials and Nanosystems for Biomedical Applications: An Overview of Liposome-Derived Nanocarrier Technologies*; Springer Books, 2007; pp 113−123.

(2) Mozafari, M. R. *Nanocarrier Technologies Frontiers in Nanotechnology: Bioactive Entrapement and Targeting Using Nanocarrier Technologies: An Introduction*; Springer Books, 2006; pp 1−16.
(3) Sharma, A.; Sharma, U. *Int. J. Pharm.* **1997**, *154*, 123–140.
(4) Michel, M.; Vautier, D.; Voegel, J.-C.; Schaaf, P.; Ball, V. *Langmuir* **2004**, *20*, 4835–4839.
(5) Volodkin, D. V.; Arntz, Y.; Schaaf, P.; Moehwald, H.; Voegel, J.-C.; Ball, V. *Soft Matter* **2008**, *4*, 122.
(6) Schlenoff, J. B.; Dubas, S. T.; Farhat, T. *Langmuir* **2000**, *16*, 9968–9969.
(7) Michel, M.; Arntz, Y.; Fleith, G.; Toquant, J.; Haikel, Y.; Voegel, J.-C.; Schaaf, P.; Ball, V. *Langmuir* **2006**, *22*, 2358–2364.
(8) Michel, A.; Izquierdo, A.; Decher, G.; Voegel, J.-C.; Schaaf, P.; Ball, V. *Langmuir* **2005**, *21*, 7854–7859.
(9) Volodkin, D. V.; Schaaf, P.; Moehwald, H.; Voegel, J.-C.; Ball, V. *Soft Matter* **2009**, *5*, 1394–1405.
(10) Kumar, K.; Tang, C. S.; Rossetti, F. F.; Textor, M.; Keller, B.; Vörös, J.; Reimhult, E. *Lab. Chip.* **2009**, *9*, 718–725.
(11) Graf, N.; Albertini, F.; Petit, T.; Reimhult, E.; Vörös, J.; Zambelli, T. *Adv. Funct. Mater.* **2011**, *21*, 1666–1672.
(12) Lynge, M. E.; Ogaki, R.; Laursen, A. O.; Lovmand, J.; Sutherland, D. S.; Städler, B. *ACS Appl. Mater. Interfaces* **2011**, *3*, 2142–2147.
(13) Granéli, A.; Benkoski, J.; Höök, F. *Anal. Biochem.* **2007**, *367*, 87–94.
(14) Granéli, A.; Edvardsson, M.; Höök, F. *ChemPhysChem* **2004**, *5*, 729–733.
(15) Bürgel, S. C.; Guillaume-Gentil, O.; Zheng, L.; Vörös, J.; Bally, M. *Langmuir* **2010**, *26*, 10995–11002.
(16) Picart, C.; Mutterer, J.; Richert, L.; Luo, Y.; Prestwich, G. D.; Schaaf, P.; Voegel, J.-C.; Lavalle, P. *Proc. Natl. Acad. Sci. U.S.A.* **2002**, *99*, 12531–12535.
(17) Izquierdo, A.; Ono, S.; Voegel, J.-C.; Schaaf, P.; Decher, G. *Langmuir* **2005**, *21*, 7558–7567.
(18) Guillaume-Gentil, O.; Graf, N.; Boulmedais, F.; Schaaf, P.; Vörös, J.; Zambelli, T. *Soft Matter* **2010**, *6*, 4246–4254.
(19) Rodahl, M.; Kasemo, B. *Rev. Sci. Instrum.* **1996**, *67*, 3238–3241.
(20) Grieshaber, D.; MacKenzie, R.; Vörös, J.; Reimhult, E. *Sensors* **2008**, *8*, 1400–1458.
(21) Guillaume-Gentil, O.; Abbruzzese, D.; Thomasson, E.; Vörös, J.; Zambelli, T. *ACS Appl. Mater. Interfaces* **2010**, *2*, 3525–3531.
(22) Tezcaner, A.; Hicks, D.; Boulmedais, F.; Sahel, J.; Schaaf, P.; Voegel, J.-C.; Lavalle, P. *Biomacromolecules* **2006**, *7*, 86–94.
(23) Richert, L.; Engler, A.; Discher, D.; Picart, C. *Biomacromolecules* **2004**, 1908–1916.
(24) Mjahed, H.; Voegel, J.-C.; Senger, B.; Chassepot, A.; Rameau, A.; Ball, V.; Schaaf, P.; Boulmedais, F. *Soft Matter* **2009**, *5*, 2269.
(25) Wood, K. C.; Chuang, H. F.; Batten, R. D.; Lynn, D. M.; Hammond, P. T. *Proc. Natl. Acad. Sci. U.S.A.* **2006**, *103*, 10207–10212.